$\pi-\pi$ and $\sigma-\pi$ Interactions in α,ω-Di-(9-anthryl) and Di-(1-naphthyl) Oligosilanes Studied by Time-Resolved Fluorescence in Solution

Takashi Karatsu,*,† Toshifumi Shibata,† Atsuko Nishigaki,† Akihide Kitamura,*,† Yusuke Hatanaka,‡ Yoshinobu Nishimura,‡ Shin-ichiro Sato,‡ and Iwao Yamazaki*,‡

Department of Materials Technology, Faculty of Engineering, Chiba University, 1-33 Yayoi-cho, Inage-ku, Chiba 263-8522, Japan, and Graduate School of Engineering, Hokkaido University, Sapporo 060-8628, Japan

Received: June 4, 2003; In Final Form: September 4, 2003

The photophysical properties of two series of oligosilanes, (1-naphthyl)-$(SiMe_2)_n$-(1-naphthyl) (**1**−**5**) and (9-anthryl)-$(SiMe_2)_n$-(9-anthryl) (**6**−**10**) with $n = 1-4$ and 6, were investigated. In these compounds, two types of interactions, a $\pi-\pi$ interaction between two aromatic groups and a $\sigma-\pi$ interaction between aromatics and a silicon chain unit, were observed. Intramolecular excimer emission was observed in cyclohexane when $n \geq 2$. The strongest excimer emission of **2** and **7** is different from the Hirayama rule ($n = 3$) proposed for carbon analogues and also shows that intramolecular cycloaddition is minor. The time-resolved fluorescence spectra of an anthryl series revealed that the time constant of excimer formation varied depending on the chain length (82−152 ps). In the cases of **4**, **5**, and **10**, charge-transfer (CT) emission was observed in acetonitrile or THF. The time constant of the CT-state formation for **10** was relatively slow (45 ps), which may indicate a conformational change. Monomer emission from the locally excited state was observed for **1** and **6** in both cyclohexane and acetonitrile.

Introduction

α,ω diaryl oligosilanes have attracted much attention because they have interesting photochemical characteristics compared to those of the carbon chain analogues.[1−4] Di-(9-anthryl)-dimethylsilane (**5**) is reported to produce unique [4 + 2] cycloadducts,[1] which are very similar to the photoadduct produced by the bis-9-anthrylethylenes.[5] The α,ω bis-3-pyrenyl oligosilanes are also reported to produce excimer emission by photoexcitation.[3] In that report, two pyrenyl groups are proposed to interact even in the ground-state-based chemical shift of the ^{1}H NMR spectra, and a strong excimer emission was observed in the case of the disilane unit as a linker. It is to be noted that a charge-transfer (CT) state of diaryloligosilanes is formed in addition to excimer formation. The direction of CT between the aromatic group and disilane unit is a subject of controversy.[6−10]

In this report, we examined the photophysical properties of the α,ω di-(1-naphthyl) and di-(9-anthryl) oligosilanes [Np-$(SiMe_2)_n$-Np (**1**−**5**), Ant-$(SiMe_2)_n$-Ant (**6**−**10**), $n = 1-4$ and 6] (Figure 1) in which $\pi-\pi$ interactions between the two aryl groups and $\sigma-\pi$ interactions between the aryl group and the silicon chain unit are expected to occur. It is very important to compare the ability of the $\pi-\pi$ interaction of these compounds with those of a carbon chain analogue. Although a compound with a carbon chain length of $n = 3$ is known to have the highest ability to produce an excimer (known as the Hirayama rule, Figure 2),[11] 1,3-di-(9-anthryl)propane does not produce efficient excimer emission because the excimer is the key intermediate to give the [4 + 4] cycloadduct.[12−14] The bond length of the Si−Si or S−C bond is longer than the C−C bond; therefore, the conformations before and after making the excimer should be very different. In addition, changing the silane chain lengths

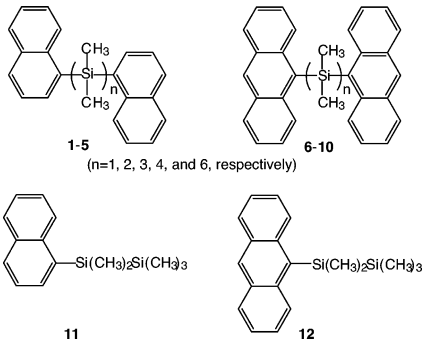

Figure 1. Di-(1-naphthyl) and di-(9-anthryl) oligosilanes evaluated in this study.

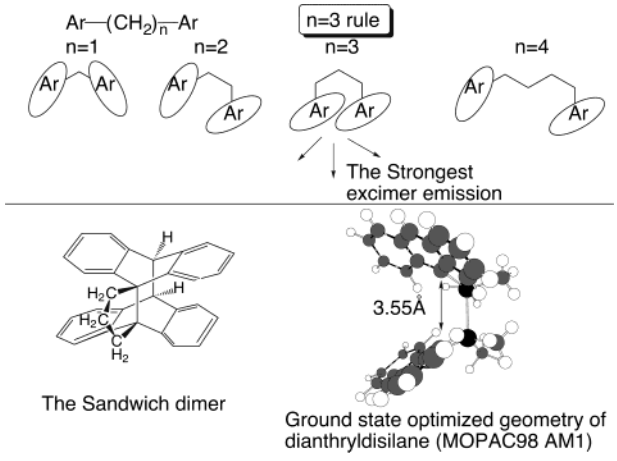

Figure 2. Hirayama rule (top) and the sandwich dimer of di-(9-anthryl)-propane (bottom left). Calculated structure of **6** (bottom right).

* To whom correspondence should be addressed. E-mail: karatsu@faculty.chiba-u.jp. Phone: +81-43-290-3366. Fax: +81-43-290-3039.
† Chiba University.
‡ Hokkaido University.

10.1021/jp0355760 CCC: $25.00
Published on Web 10/11/2003

makes it easier to change the oxidative and reductive energy levels versus the aromatic energy level. This may allow one to understand the mechanism of CT-state formation.

Experimental Section

Compounds **1**−**10** were prepared from 1-naphthyllithium and 9-anthryllithium (obtained from aryl bromide and 1.6 M *n*-butyllithium in hexane) and 1,*n*-dichloropermethyloligosilanes (Cl-$(SiMe_2)_n$-Cl). The 1,2-dichlorotetramethyldisilane ($n = 2$) was purchased from Tokyo Kasei, and the other dichlorotri-, dichlorotetra-, and dichlorohexasilanes ($n = 3$, 4, 6) were synthesized from dodecamethylcyclohexasilane and pentachlorophosphine as previously reported.[15] 1-Pentamethyl-disilylnaphthalene (**11**) and 9-pentamethyldisilylanthracene (**12**) were synthesized from the lithio-aromatics and chloropentamethyldisilane. The chloride was prepared by the reaction of ammonium chloride with a hexamethyldisilane and sulfuric acid mixture as previously reported.[16] All of the compounds were characterized using a JEOL SX-400 ^{1}H NMR spectrometer.

The absorption spectra and steady-state fluorescence spectra were measured using Hitachi U-3000, Hitachi F-4010, and JASCO FP6600 spectrophotometers.

The molecular orbital calculation was performed by MOPAC 98.[17]

The fluorescence decay curves and time-resolved fluorescence spectra were measured with a picosecond pulse laser and a single-photon timing apparatus at Hokkaido University.[18] The laser system was a mode-locked Ti:sapphire laser (Coherent, Mira 900) pumped by an argon ion laser (Coherent, Innova 300) combined with a pulse picker (Coherent, model 9200, repetition rate 2.9 MHz). The third harmonics (280 nm) generated by an ultrafast harmonic system (Inrad, model 5-050) were used as the excitation light source. The decay curve was obtained by monitoring the emission with a microchannel-plate photomultiplier (Hamamatsu R2809U-01). The pulse width of the instrumental response function was 30 ps (fwhm). The picosecond time-resolved fluorescence spectra were obtained from the decay curves monitored at different wavelengths ranging from 300 to 600 nm with a 0.625-nm step. The time-resolved spectrum was constructed from a series of decay curves by plotting the fluorescence (FL) intensities at the given delay times as a function of the emission wavelength. The time constant of the rise-up excimer component was obtained from the plots of excimer emission intensities measured from the time-resolved FL spectra versus time after the laser pulses.

Results and Discussion

Ground-State Conformation Studied by ^{1}H NMR and MO Calculations. The ground-state conformations for **1**−**10** were considered by the chemical shift of the ^{1}H NMR spectra. For all of the 1-naphthyl and 9-anthryl compounds, eight and five aromatic proton signals and one to three singlet methyl signals from the dimethylsilyl units were observed. Figure 3 shows the change in the chemical shift of the aromatic signals with silicon chain length. The aromatic signals appeared as a singlet or complicated coupling signals,indicating that a rapid rotation along the Si−C or Si−Si bonds made the methyl groups and two aromatic environments equivalent. In both series of naphthyl or anthryl silanes, chemical shifts for the compounds with chain lengths of two and three appeared in a higher magnetic field region than those of the other compounds. For example, H at positions 2−8 on a naphthalene ring were observed at 7.80, 7.20, 7.80, 7.57, 7.39, 7.39, 7.80 ppm for **2** and at 7.84, 7.46, 7.84, 7.63, 7.46, 7.46, 7.98 ppm for 1-(pentamethyldisilyl)-naphthalene (**11**), respectively. For the anthryl derivatives, H at the 1, 4, 3, 2, and 10 positions of 9-(pentamethyldisilyl)-anthracene (**12**) were observed at 7.42, 7.44, 8.00, 8.34, 8.43 ppm, respectively, and at 7.13, 7.35, 7.95, 8.24, and 8.40 ppm, respectively, for **7**. The signals of **1**, **4**−**6**, **9**, and **10** appeared at similar positions to the signals of disilanylaromatics **11** and **12**, respectively. This indicates that the contribution of a sandwich-type conformer in a ground-state conformational equilibrium is very small.

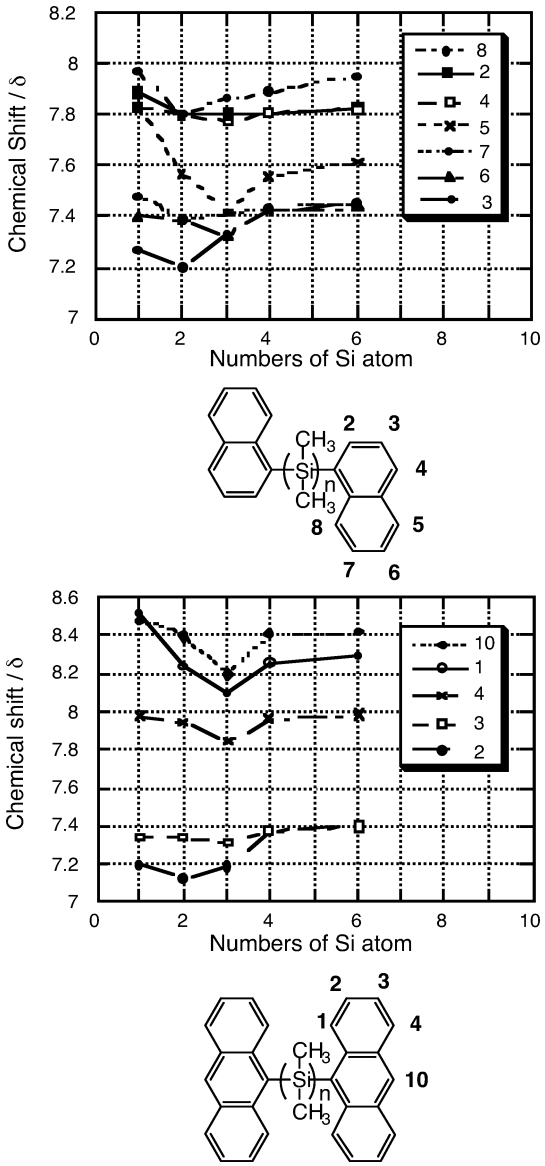

Figure 3. ^{1}H NMR chemical shift of di-(1-naphthyl) and di-(9-anthryl) oligosilanes.

The ground-state potential energy surface of rotamerism was calculated by the MOPAC98/PM3 method. The calculation of phenylpentamethyldisilane has been reported using a more reliable method (CASSCF6-31G*);[7c] however, the molecules here are too large to use such a basis set. The Si−C and Si−Si bonds are longer; therefore, the activation energy for rotation should be smaller than the C−C bond energy. Figure 4 shows the calculated potential energy surfaces of rotation around the Si−Si bonds of **2**, **7**, **11**, and **12** and their carbon chain analogues. The optimized structure has a Si−Si bond perpendicular to the aromatic plane, which is favorable for $\sigma-\pi$ interactions between π orbitals of aromatics and σ orbitals of

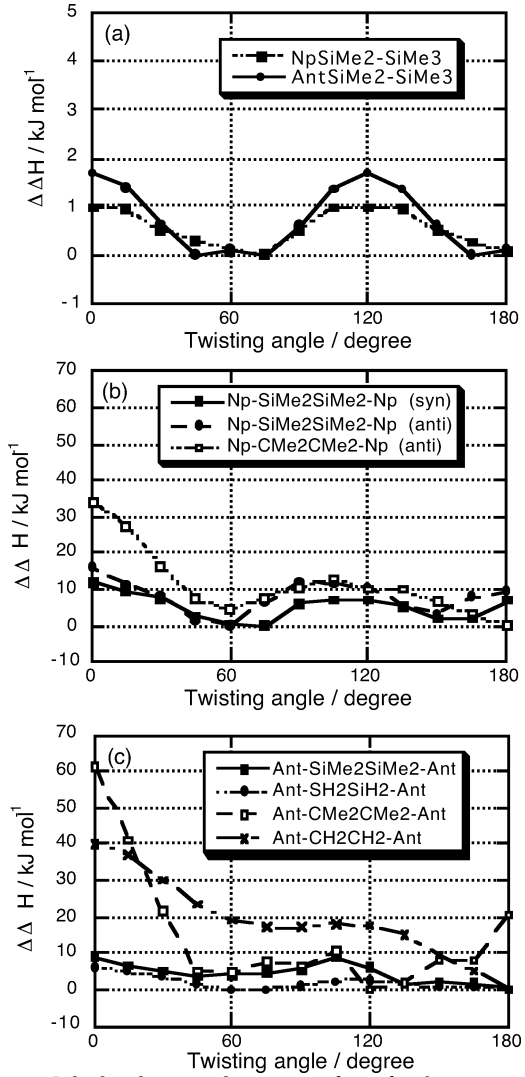

Figure 4. Calculated potential energy surfaces for the rotation of the Si−Si bond (PM3) of (a) **11** (circles) and **12** (squares), (b) **2**, and (c) **6** and their carbon chain analogues.

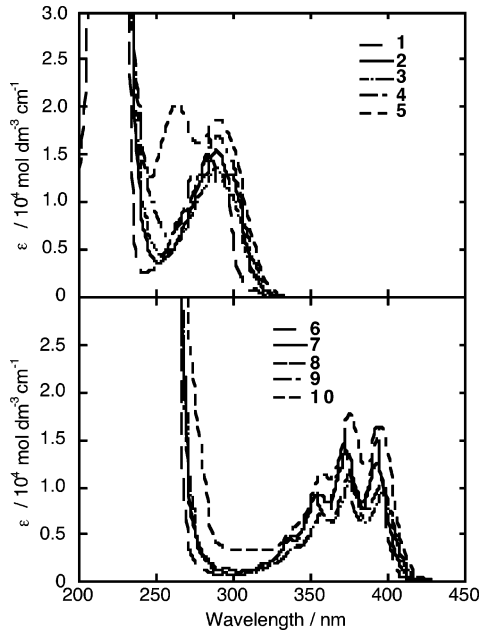

Figure 5. Absorption spectra of **1**−**5** and **6**−**10** in c-hexane.

the S−Si bond. The activation energies for the rotation of the Si−Si bond for **11** and **12** were calculated to be 1.3 and 2.1 kJ

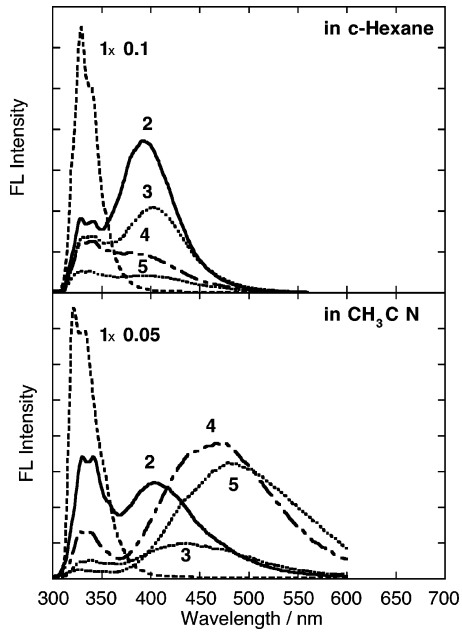

Figure 6. Fluorescence spectra of **1**−**5** in deaerated c-hexane and acetonitrile.

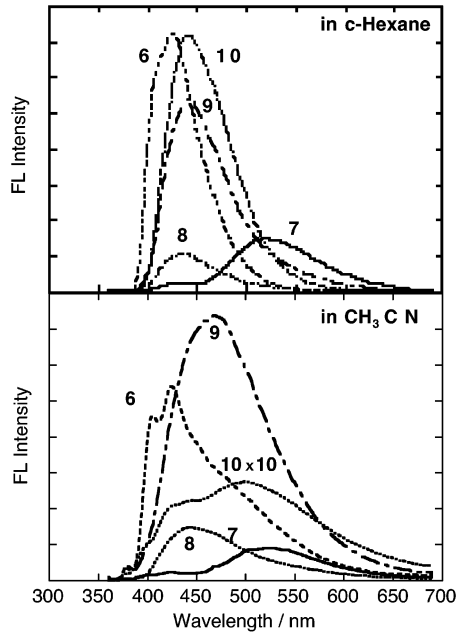

Figure 7. Fluorescence spectra of **6**−**10** in deaerated c-hexane and acetonitrile.

mol^{-1}, respectively (Figure 4a). They are much smaller than the value of 17 kJ mol^{-1} calculated for 1-naphthylCMe$_2$−CMe$_3$.

In addition, conformations were considered for **2** and **7** by PM3. The potential energy surfaces of rotation around the Si−Si bond were compared with those of carbon analogues as shown in Figure 4b and c. For **2**, two isomeric conformers exist depending on the orientation of the two 1-naphthyl groups. One is that two naphthyl groups stack on top of each other by only one benzene ring when two Si−C bonds take an eclipsed conformation to each other. This structure has a C_2 axis perpendicular between the Si−Si bonds. The eclipsed conformer of another series has a structure such that two naphthyl groups can completely stack face-to-face; therefore, it has mirror plane symmetry (C_{2v}). The former and latter series are expressed as anti and syn, respectively, in Figure 4b. The rotational barrier for the C−C bond with the eclipsed conformation of two

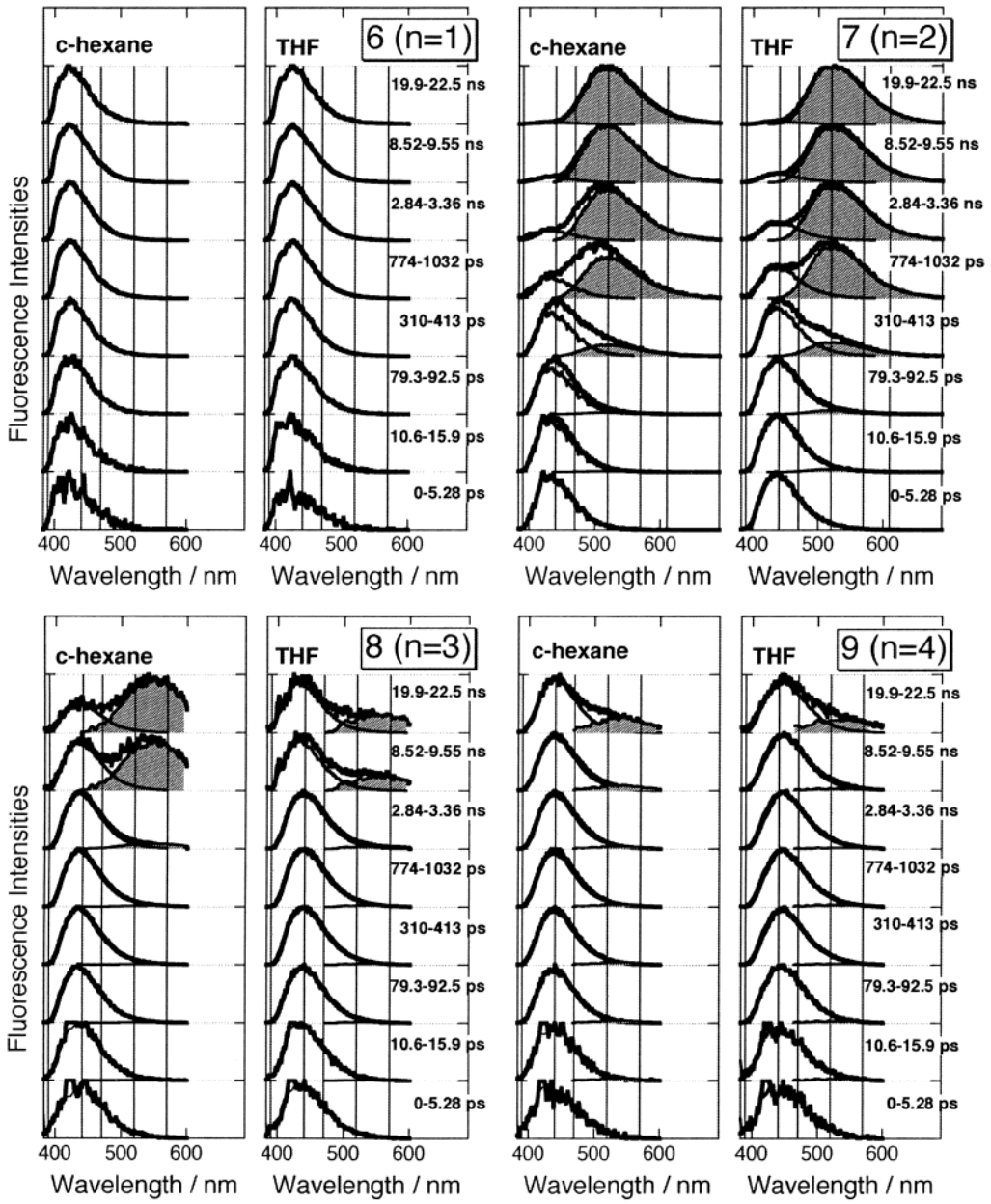

Figure 8. Time-resolved fluorescence spectra of **6**−**9** in cyclohexane and THF.

TABLE 1: Calculated Heat of Formation ($\Delta\Delta H$/kJ mol^{-1}) for the Conformers of 8 by the PM3 Method

	t	g^+	g^-
t	tt = 0	$g^+ = 0.4$	$g^- = 0.4$
g^+	g^+	gg = 18.1	$g^+g^- = 8.8$
g^-	g^-	g^+g^-	gg = 18.1

1-naphthyl groups is twice as high as that for the Si−Si bond. This barrier becomes much higher for 1,2-di(9-anthryl)ethane as shown in Figure 4c. The optimized structures of **7**, **8**, and **12** described above are similar to the recently reported structures determined by X-ray crystallography.[19]

The heat of formation energies for the stable conformers consisting of Si−Si−Si bonds of **8** were calculated as shown in Table 1. The tt conformer is used as the starting conformer. One of the Si−Si bonds is then twisted clockwise or counterclockwise to make two gauche conformers, g^+ and g^-. Similarly, the gg and g^+ g^- conformers were made and optimized by the PM3 method. There are almost no differences in energy between the anti, g^+, and g^- conformers; however, there is a significant difference between gg and g^+g^-. A weak excimer fluorescence of **8** is explained by the small population of the conformers that leads to the excimer in equilibrium in the ground state and the long distance between intramolecular chromophores due to the long Si−Si bond length of the excimer.

Absorption and Steady-State Fluorescence Measurement. Figure 5a and b indicates the absorption spectra of **1**−**5** and **6**−**10** in cyclohexane and acetonitrile, respectively. The absorption spectra of **1**−**5** and **6**−**10** are shifted about 15 nm to longer wavelengths than that of naphthalene or anthracene. They are very similar to each other, indicating neither a strong interaction between the two aromatic chromophores nor a dependence of the σ conjugation on the chain length. For **5** and **10**, the absorption band assigned to the hexasilyl group appeared at around 260 nm, and this is evident for **5**. From the ^{1}H NMR analysis, compounds with $n = 2$ to 3 show a weak interaction between the two overlapping aromatic rings, as indicated by the higher field shifts of the aromatic protons as mentioned above.

Figures 6 and 7 show the fluorescence spectra of **1**−**5** and **5**−**10**, respectively, in cyclohexane and acetonitrile. Compounds

TABLE 2: Time Constant of Decay and Rise-up Components of the Fluorescence of 6-9[a]

	in c-hexane		in THF	
compds	420 nm	520 nm	420 nm	520 nm
6	4.90	5.60	4.96	5.63
7	82.1 ps + 248 ps + 7.76	−74.4 ps + 260 ps + 7.30	99.8 ps + 5.07 + 20.6	−85.0 ps + 5.32 + 19.1
8	126 ps + 1.55	−92.6 ps + 1.28	122 ps + 9.47	−98.8 ps + 7.71
9	152 ps + 2.82	−152 ps + 2.81	141 ps + 17.8	−116 ps + 8.30

[a] Values without units are presented in ns, and negative values at 520 nm are rise-up components.

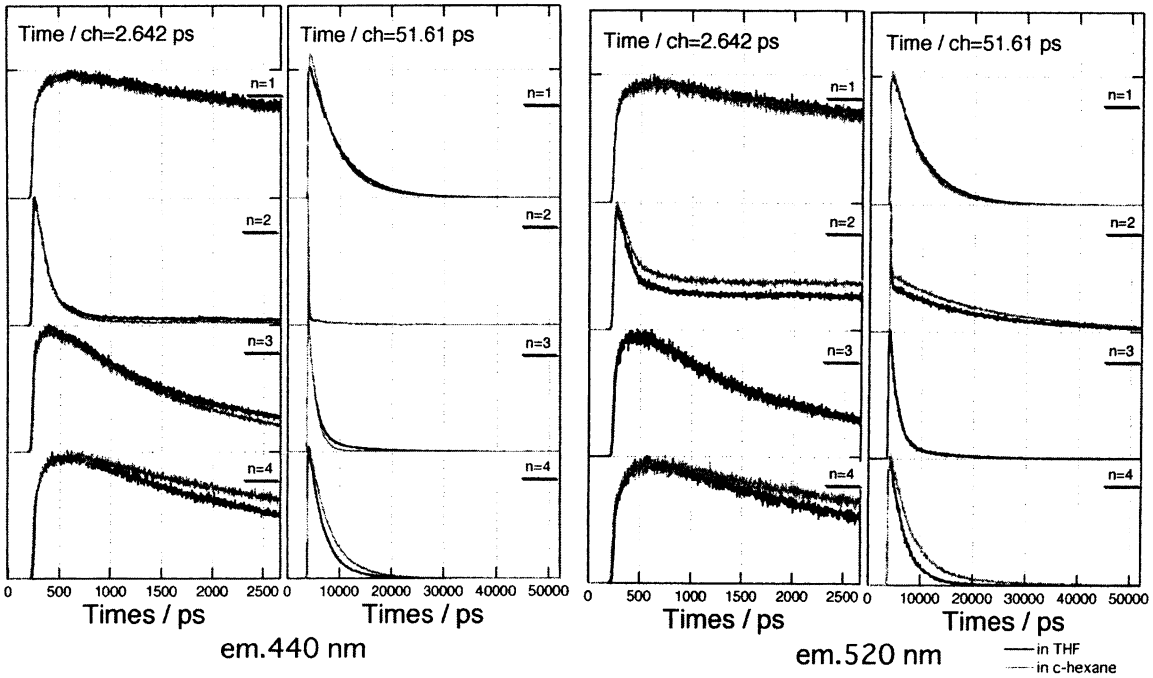

Figure 9. Decay profiles of the fluorescence spectra of **6**−**9** observed at 440 and 520 nm in cyclohexane and THF.

1 and **5** produced only monomer-like fluorescence in both solvents. However, a silicon chain length of more than 2 showed excimer emission in cyclohexane. For **2**−**5**, the intensity of the excimer emission decreased with increasing chain length in cyclohexane. For **6**−**10**, the fluorescence behavior is somewhat different from that of **1**−**5**. Excimer emission with a large Stokes shift was observed for **7** (Figure 5a). This shift (λ_{max} = 520 nm) is much larger than those observed for **8** and **9**, indicating the closely stacked conformation of **7** in its excimer. Steric hindrance between the anthryl groups and dimethylsilane chain unit may interrupt the conformation to produce close stacking for **8** and **9**. The λ_{max} values at 620, 570, and 460 nm for the excimer emission were reported for anthracenophanes with 1, 2, and 3 phenyl rings in anthracene stacked face-to-face, respectively.[20] In addition, there is the Hirayama rule that states that an excimer is most stable with a three-carbon chain unit; 1,3-di(9-anthryl)propane undergoes efficient [4 + 4] cycloaddition showing no excimer emission.[13,14] In our case, **7** has unique characteristics in which the Si−Si bond is longer than the C−C bond; the two anthracene rings produce sandwich-like stacking with a large distance between the 9−9′ positions and a larger distance between the 10−10′ positions. The nearest distance between the 9−9′ positions is calculated to be 3.55 Å by the PM3 method for the eclipsed conformation of the ground state (**7**) as shown in Figure 2 (bottom right). Therefore, it has a strong excimer emission without undergoing efficient photocyclization. This may be attributed to two reasons: (1) a fairly long Si−Si bond length provides an appropriate distance between the two anthracene rings for excimer formation and (2) the conformation of the central Si−Si bond is restricted to gauche by the steric hindrance of the methyl substitutions on the Si atoms.

Solvent Effect and CT Emission. The λ_{max} of the emission of **1**−**3** and **5**−**9** in acetonitrile did not show a significant difference from that in cyclohexane. However, the λ_{max} of the emission of **4**, **5**, and **10** shifted to longer wavelengths in acetonitrile than in cyclohexane. These shifts were quite different from those observed for the excimer emissions of **2** and **7**. The emission that showed a large shift can be assigned to the CT emission because excimer emission does not show such a large shift.

There have been many studies on the CT mechanism of aryl disilanes.[6−10] In our experiment, the CT emission band was observed for the naphthylsilanes with $n > 3$ but was not observed in the case of anthrylsilanes for $1 < n < 4$ in a polar solvent. These results are consistent with the mechanism proposed by the $\sigma \rightarrow \pi^*$ OICT mechanism,[8,9] where CT occurred from the silane to the aryl unit. The electron-donating ability of the silane unit increases with increasing chain length, and the electron-accepting ability of the anthryl group is lower than that of the naphthyl group. Another mechanism of $2p\pi^* \rightarrow 3d\pi$[6,7] is proposed as a alternative mechanism for the phenyldisilane derivatives, and this mechanism does not seem to contradict the experimental result. However, note that the π^*-state energy level of the naphthyl moiety is higher than that of the anthryl moiety and that the energy of the $3d\pi$ state decreases with increasing silane chain length. Also noteworthy is that the energy of the $3d\pi$ state of the silane is expected to be higher than that of the $2p\pi^*$ state of naphthalene. It follows that as a favorable mechanism charge transfer occurs from the

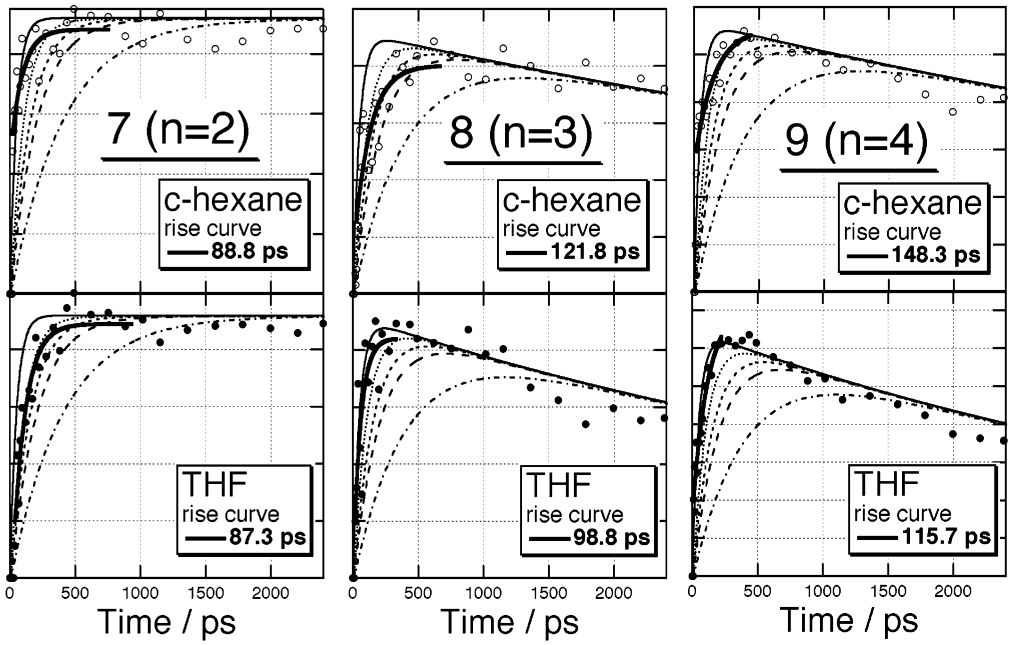

Figure 10. Extraction of the rise-up components from the fluorescence spectra of **7**−**9**. The observed points of the rise-up and simulation curves of 50 (−), 100 (···), 150 (- - -), 200 (− − −), and 400 ps (− · − ·), respectively. The bold lines were fitted using a nonlinear least-squares fitting method.

silane unit to the naphthyl or anthryl group. The OICT mechanism of $\sigma \rightarrow \pi^*$[8,9] may also be appropriate, at least in these cases.

Time-Resolved Fluorescence Measurement. The time-resolved fluorescence spectra and their time profiles are shown in Figures 8 and 9, respectively. The spectra are normalized at the maximum wavelength. The spectra of **6** did not change with time and decayed with the lifetimes of 4.90 and 5.60 ns (440 nm) in c-hexane and THF, respectively. For compounds **7** and **8**, the FL maxima are shifted to longer wavelengths in the later time region. The maxima are shifted to 520 and 550 nm for **7** and **8**, respectively. For compounds **7**−**9**, the rise-up components were extracted from the spectra. The excimer component was estimated by the method in which the monomer emission observed just after laser excitation was subtracted from each spectrum (Figure 8). The obtained intensities (I) of the excimer emission at λ_{max} were plotted versus time (Figure 10). The Figures show the curves fitted using a nonlinear least-squares method and the simulation curves using various time constants (50, 100, 150, 200, and 400 ps). For compound **7** in c-hexane, the fluorescence around 440 nm decays in three components: a fast-decaying component with a 100-ps lifetime, an intermediate decay component with 248-ps lifetime, and a long component with a 7.76-ns lifetime. However, the fluorescence at 520 nm is composed of a rising component with a 100-ps rise time and decay components of 5.07 and 20.6 ns. The two long-lived components may imply the existence of two kinds of excimers. These behaviors are very similar in THF. The spectra of **8** in c-hexane did not significantly change but showed only a small increase in the intensities around 550 nm. The fluorescence at 440 nm decays with lifetimes of 126 ps and 1.55 ns, and the emission at 520 nm rises with a 122-ps rise time and decays with a 9.47-ns lifetime. The spectral behavior of **9** was similar to that of **8**. These fast decay of the monomer FL and the rise of the excimer FL are consistent with excimer formation. The time constants showed almost no solvent dependence.

The time-resolved fluorescence indicates that the conformers produce excimer emission from a weakly coupled dimer, even in the ground state, because excimer emission rapidly rises just after excitation. This result is consistent with the result from the ^{1}H NMR analysis for the ground-state conformation mentioned above. The FL quantum yields (Φ_f) for **6**−**10** were 0.40, 0.07, 0.05, 0.35, and 0.40, respectively, and these values may partially reflect the inverse population of the sandwich-like conformers in the ground state.

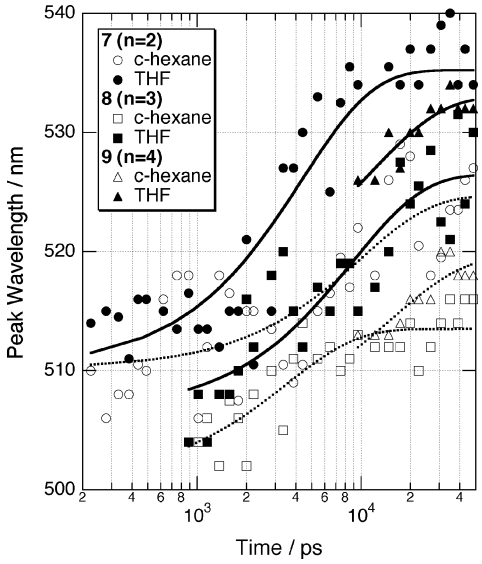

Figure 11. Time and solvent dependence of the shift of the excimer emission λ_{max} for **7**−**9**.

Figure 11 shows that the excimer FL λ_{max} shift occurred on a slower time scale after laser excitation. These shifts were between 10 and 25 nm and occurred on the 20-ns time scale depending on the chain lengths and solvents. The absolute shifts are greater in THF than in c-hexane, indicating more stabilizing excimer formation in THF than in c-hexane. The time scale of this phenomenon is much slower than that observed in the picosecond time frame mentioned above.

Figure 12 shows the time-resolved fluorescence spectra of **10** in c-hexane and acetonitrile. **10** is the only compound in which CT emission was observed in acetonitrile by a steady-

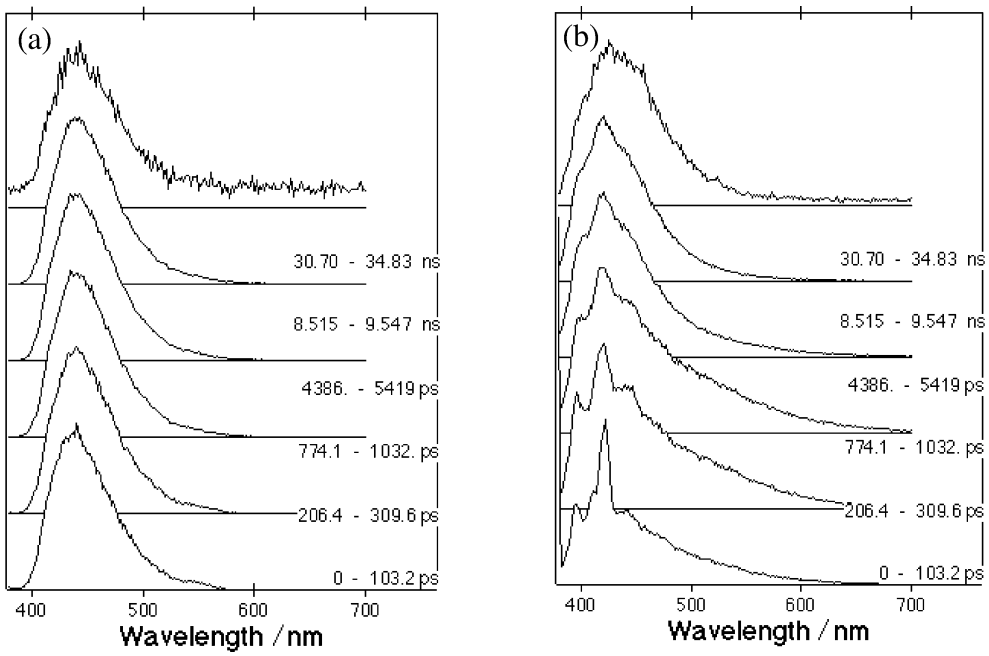

Figure 12. Time-resolved spectra of **10** in (a) c-hexane and (b) acetonitrile.

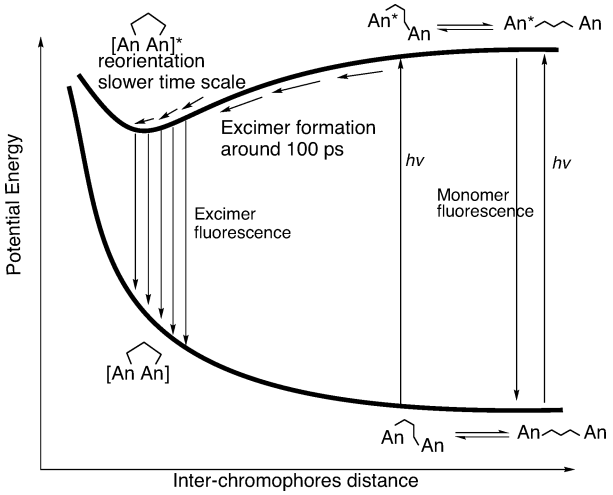

Figure 13. Proposed potential energy surface of excimer formation.

state fluorescence measurement in the di-(9-anthryl)-oligosilane series. The spectra did not show any change between just after the laser excitation and 35 ns, indicating a very small contribution of the excimer formation in c-hexane. However, in acetonitrile, the time-resolved spectra showed a time dependence, and the fluorescence decayed in three components: 45 ps and 1.72 and 5.6 ns at $\lambda_{obs} = 440$ nm, with an observed 47-ps rise-up and a 5.0-ns decay at $\lambda_{obs} = 570$ nm. The picosecond time scale change must be attributed to the CT process, and this process may require a conformational change as proposed by the OICT mechanism.[9,10]

Figure 13 shows a schematic representation of the potential energy surfaces of the ground state and the excited-state excimer formation. The excimer-formation process might involve two processes having different time orders. The first process is a fast process of around 100 ps corresponding to excimer formation from the Franck−Condon state; however, this process may occur for the conformer that has a sandwich-like conformation in the ground state. The second process might be a stabilizing process including a solvent reorientation similar to the reported TICT of bianthryl.[21] The formation of the excimer induces reorientations of the solvent molecules and then more stabilization of the excimer structure. This is more effective in a polar solvent than in a nonpolar solvent as observed here. This process might be slow because it accompanies the reorientations of a large number of solvent molecules and a readjustment of the face-to-face excimer. This process is slow like the motion of two magnets after they have attracted each other.

Conclusions

In conclusion, for the **2**−**5** and **7**−**10** cases, intramolecular excimer emissions were observed in cyclohexane, and the strongest excimer fluorescence was observed for **2** and **7** (chain length $n = 2$). CT emission was observed for **4**, **5**, and **10**, indicating charge transfer from the silane unit to the naphthyl or anthryl group and suggesting a $\sigma-\pi$ interaction in acetonitrile. Only excimer emission was observed for **2**, **3**, and **7**−**9** in acetonitrile as similarly seen in cyclohexane. Only monomer-type emission was observed for **1** and **6** in both cyclohexane and acetonitrile. The time-resolved fluorescence measurements showed that the excimer fluorescence rise-up times (about 90, 120, 140 ps for **7**−**9**, respectively) were weakly time-dependent and independent of the solvent viscosity and polarity. These results reveals that the average conformation is more stretched for the longer-chain compounds; however, there is a significant population of conformers that already have a weak interaction in the ground state. In acetonitrile, the CT fluorescence rise time was 45 ps, indicating a rapid conformational transformation from the Franck−Condon state to the CT state.

Acknowledgment. This work was supported by Grants-in-Aid for Scientific Research on Priority Areas (417, no. 14050022) and Scientific Research (no. 14550786) from the Ministry of Education, Culture, Sports, Science, and Technology (MEXT) of the Japanese Government to T.K.

References and Notes

(1) (a) Sakurai, H.; Sakamoto, K.; Nakadaira, A.; Kira, M. *Chem. Lett.* **1985**, 497. (b) Daney, M.; Vanucci, C.; Desvergne, J.-P.; Castellan, A.; Bouas-Laurent, H. *Tetrahedron Lett.* **1985**, *26*, 1505.

(2) Pitt, C. G.; Carey, R. N.; Toren, E. C., Jr. *J. Am. Chem. Soc*. **1972**, *94*, 3806.

(3) (a) Declercq, D.; Delbeke, P.; de Schryver, F. C.; Meervelt, L. V.; Miller, R. D. *J. Am. Chem. Soc.* **1993**, *115*, 5702. (b) Declercq, D.; de Schryver, F. C. Miller, R. D. *Chem. Phys. Lett.* **1991**, *186*, 467. (c) Declercq, D.; Hermans, E.; de Schryver, F. C. Miller, R. D. *Proc. − Indian Acad. Sci., Chem. Sci.* **1993**, *105*, 451.

(4) (a) Karatsu, T.; Shibata, T.; Nishigaki, A.; Fukui, K.; Kitamura, A. *Chem. Lett.* **2001**, 994. (b) Fang, M.-C.; Watanabe, A.; Matsuda, M. *Macromolecules* **1996**, *29*, 6807.

(5) Becker, H.-D. *Advances in Photochemistry*; Volman, D. H., Hammond, G. S., Gollnick, K., Eds.; Wiley & Sons: New York, 1990; Vol. 15, pp 139−227.

(6) Pitt, C. G.; Carey, R. N.; Toren, E. C., Jr. *J. Am. Chem. Soc*. **1972**, *94*, 3806.

(7) (a) Shizuka, H.; Sato, Y.; Ueki, Y.; Ishikawa, M.; Kumada, M. *J. Chem. Soc., Faraday Trans. 1* **1984**, *80*, 341. (b) Shizuka, H.; Okazaki, K.; Tanaka, M.; Ishikawa, M.; Sumitani, M.; Yoshihara, K. *Chem Phys. Lett*. **1985**, *113*, 89. (c) Yamamoto, M.; Kudo, T.; Ishikawa, M.; Tobita, S.; Shizuka, H. *J. Phys. Chem. A* **1999**, *103*, 3144.

(8) Horn, K. A.; Grossman, R. B.; Throne, J. R. G.; Whitenack, A. A. *J. Am. Chem. Soc.* **1989**, *111*, 4809.

(9) (a) Kira, M.; Miyazawa, T.; Sugiyama, H.; Yamaguchi, M.; Sakurai, H. *J. Am. Chem. Soc.* **1993**, *115*, 3116. (b) Sakurai, H.; Sugiyama, H.; Kira, M. *J. Phys. Chem.* **1990**, *94*, 1837. (c) Tajima, Y.; Ishikawa, H.; Miyazawa, T.; Kira, M.; Mikami, N. *J. Am. Chem. Soc.* **1997**, *119*, 7400.

(10) (a) Sakurai, H.; Kira, M. *J. Am. Chem. Soc.* **1974**, *96*, 791. (b) Sakurai, H.; Kira, M. *J. Am. Chem. Soc*. **1975**, *97*, 4879.

(11) Hirayama, F. *J. Chem. Phys.* **1965**, *42*, 3163.

(12) Bouras-Laurent, H.; Desvergne, J.-P. *Photochromism*; Dürr, H., Bouras-Laurent, H., Eds.; Elsevier: Amsterdam, 1990; Chapter 14, pp 561−630 and references therein.

(13) Bouas-Laurent, H.; Castellan, A.; Desvergne, J.-P. *Pure Appl. Chem.* **1980**, *52*, 2633.

(14) Bergmark, W. R.; Jones, G., II; Reinhardt, Th. E.; Halpern, A. M. *J. Am. Chem. Soc*. **1978**, *100*, 6665.

(15) Gilman, H.; Inoue, S. *J. Org. Chem.* **1964**, *29*, 3418.

(16) Kumada, M.; Yamaguchi, M.; Yamamoto, Y.; Nakajima, J.; Shiina, K. *J. Org. Chem.* **1956**, *21*, 1264.

(17) Stewart, J. J. P. *MOPAC 98*; Fujitsu Limited: Tokyo, Japan, 1998.

(18) (a) Nishimura, Y.; Yasuda, A.; Speiser, S.; Yamazaki, I. *Chem Phys. Lett*. **2000**, *323*, 117. (b) Hasegawa, M.; Enomoto, S.; Hoshi, T.; Igarashi, K.; Yamazaki, T.; Nishimura, Y.; Speiser, S.; Yamazaki, I. *J. Phys. Chem. B* **2002**, *106*, 4925.

(19) Yang, D.-D. H.; Yang, N. C.; Steele, I. M.; Li, H.; Ma, Y.-Z.; Fleming, G. R. *J. Am. Chem. Soc*. **2003**, *125*, 5107.

(20) Hayashi, T.; Mataga, N.; Sakata, Y.; Misumi, S.; Morita, M.; Tanaka, J. *J. Am. Chem. Soc*. **1976**, *98*, 5910.

(21) Kang, T. J.; Kahlow, M. A.; Giser, D.; Swallen, S.; Nagarajan, V.; Jarzeba, W.; Barbara, P. F. *J. Phys. Chem*. **1988**, *92*, 6800.